energies

MDPI

Article

Experimental Study on the Stabilization Mechanism of Diffusion Flames in a Curved Impinging Spray Combustion Field in a Narrow Region

Hideo Kawahara [1,*], Konosuke Furukawa [1], Koichiro Ogata [2], Eiji Mitani [3] and Koji Mitani [3]

[1] Department of Shipping Technology, National Institute of Technology, Oshima College, 1091-1 Komatsu, Suo Oshima, Oshima, Yamaguchi 742-2193, Japan; k610@oshima-k.ac.jp
[2] Department of Mechanical Engineering, National Institute of Technology, Oita College, 1666 Maki, Oita City 870-0152, Japan; k-ogata@oita-ct.ac.jp
[3] SSC Co., Ltd., Tomomachi Ushiroji 26-216, Fukuyama, Hiroshima 720-0202, Japan; e-mitani@ssc-hvaf.co.jp (E.M.); k-mitani@ssc-hvaf.co.jp (K.M.)
* Correspondence: kawahara@oshima-k.ac.jp; Tel.: +81-820-74-5495

Abstract: HVAF (High Velocity Air Flame) flame spraying can generate supersonic high-temperature gas jets, enabling thermal spraying at unprecedented speeds. However, there is a problem with the energy cost of this device. This study focused on combustors that used cheap liquid fuel (kerosene) as the fuel for HVAF. In this research, we have developed a compact combustor with a narrow channel as a heat source for the HVAF heat atomizer. Using this combustor, the stability of the flame formed in the combustor, the morphology of the flame, and the temperature behavior in the combustion chamber were investigated in detail. As a result, the magnitude of the swirling airflow had a great influence on the structure of the flame formed in the combustor, and the stable combustion range of the combustor could be determined. As the swirling air flow rate changes, the equivalent ratio of the entire combustor changes significantly, and the flame structure also transition from the premixed flame to the diffusion flame. From this study, it was confirmed that the temperature inside the combustor has great influence on the flame structure.

Keywords: diffusion flame; curved impinging jet combustion; narrow region; stable combustion; temperature fluctuation

Citation: Kawahara, H.; Furukawa, K.; Ogata, K.; Mitani, E.; Mitani, K. Experimental Study on the Stabilization Mechanism of Diffusion Flames in a Curved Impinging Spray Combustion Field in a Narrow Region. *Energies* **2021**, *14*, 7171. https://doi.org/10.3390/en14217171

Academic Editor: George Kosmadakis

Received: 23 August 2021
Accepted: 26 October 2021
Published: 1 November 2021

1. Introduction

Thermal spray technology is showing progress in the areas of thermal spray processes, thermal spray equipment, and thermal spray materials. Fields of application are diverse, and major progress is also being made in mass production technology, mainly in the automotive field. Due to this technical progress and broadening of applications, the characteristics required of thermal spray coatings have gone beyond simple protective functions, and various sophisticated functions are now required. HVAF (High Velocity Air-Fuel) flame thermal spraying [1], developed by Browning in the 1980s, can produce supersonic high-temperature gas jets, thus enabling thermal spraying at unprecedentedly high speeds, and this has allowed major improvements in coating quality. There are two types of HVAF thermal spraying: the type using gaseous fuels such as natural gas, propane, propylene, ethylene, acetylene, or hydrogen, and the type using liquid fuels such as kerosene. The biggest distinguishing feature in the liquid fuel case is the high particle speed, and by spraying solid particles onto a substrate at high speed, it is possible to provide coatings with compressive residual stress. Therefore, the method is outstanding for forming thick films and producing high-hardness coatings, and the thermal spray speed is also high, so the method is used for purposes such as coating large rolls in the steel and paper manufacturing fields, where thick films of high-hardness carbide cermet are used. Additionally, the fuel is liquid, and thus has the advantage of being easier to handle than

gas. With the liquid fuel method, on the other hand, there is a narrower range of thermal spray conditions for maintaining normal combustion, compared to the gas fuel method, and this has a major effect on the temperature and speed of thermal spray particles, and, as a result, on coating performance as well [2–4]. In addition, liquid fuel is sprayed in a limited space due to the size of thermal spraying equipment, and if complete combustion is not achieved, soot is also produced.

Spray combustion is widely used in combustors such as the engines of automobiles, ships, and other vehicles, gas turbine engines, and industrial furnaces. Improving combustion is a crucial point for improving the efficiency of these combustors and achieving cleaner exhaust gas, and the key here is to improve the atomization characteristics of the fuel injection valve. Methods employing liquid films are widely known as ways of promoting liquid atomization. A thin liquid film can be easily formed by using a technique where the liquid jet is made to collide with a wall surface, or a method where liquid jets are made to collide with each other. Therefore, there are high expectations for improved atomization characteristics, and a wide range of research has been carried out [5–16].

Now, let us gain a general overview of basic research on liquid film atomization. Tokuoka et al. [9] experimentally and analytically examined smooth liquid films formed by collisions between liquid jets. They carried out a detailed examination of factors such as speed distribution of liquid film, thickness distribution of liquid film, and the liquid film splitting mechanism due to the balance of surface tension and inertial force. Tanasawa et al. [10] experimentally and analytically examined liquid films formed by the collision between liquid jets. They discussed the liquid film splitting process, and derived a relation between liquid jet speed and liquid film particle size.

Now, let us conduct an overview of applied research on practical injection valves for liquid film atomization. Inamura et al. [11–13] experimentally examined liquid films formed by collision of a liquid jet with a wall surface. They carried out a detailed examination of the thickness distribution of the liquid film at the wall surface, and the size of droplets. Shiga et al. and Horikoshi et al. [14,15] experimentally examined techniques of applying liquid films formed through wall collision of liquid jets to air blast fuel injection valves for jet engines. They showed the possibility of promoting atomization in regions with low air flow velocity, which are a weak point for air blast fuel injection valves.

These studies have shown the basic characteristics of liquid film atomization, and the possibility of applying liquid film atomization to practical injection valves. In research on applications to practical injection valves in particular, researchers have considered use of liquid jets with high speeds of the order of 102 m/s [14,15]. One key to applying liquid film atomization to practical injection valves is thought to be increasing liquid jet speed. Elucidation of atomization characteristics of liquid films formed by the collision of these high-speed liquid jets is thought to be vital for applications in practical injection valves.

Menghini et al. [17] and Qian et al. [18,19] investigated the operating characteristics of combustors for biomass fuels, and the total of the equivalent ratio, excess air amount and secondary air amount is large in combustion temperature and exhaust gas characteristics, which have been shown to have an impact.

In this study, in order to promote efficient mixing of fuel and air in a limited space, we proposed an impinging spray combustor with swirl airflow, and examined the characteristics of flame stability and transition flames when the fuel flow rate and the swirl airflow rate were varied.

2. Experimental Method

2.1. Experimental Equipment

Figure 1 shows a conceptual diagram of the proposed combustor. First, the liquid fuel is injected from a fuel nozzle mounted in the radial direction of the combustor. The atomized fuel then collides with the combustor wall, and mixing with the surrounding air is started. On the other hand, the air oxidizer is supplied into the combustor from two pipes mounted in the tangential direction of the combustor, and it flows while swirling

along the combustor wall surface. The combustor we propose has a structure in which this flow of fuel spray from the radial direction of the combustor is combined with a swirl airflow that flows through the inside of the combustor. There is a possibility that, by using this combustor, liquid fuel atomization and fuel/air mixture will be promoted (greater combustor compactness), and it will be possible to freely control the flame position inside the combustor.

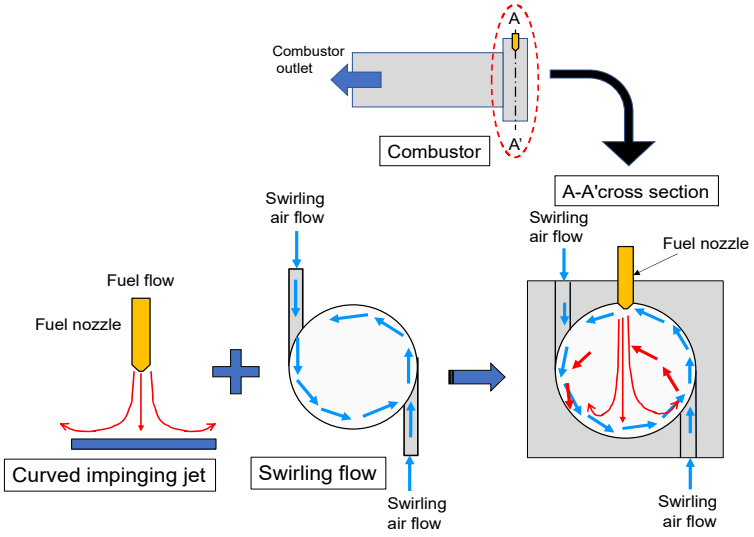

Figure 1. Conceptual diagram of the proposed combustor.

Figure 2 shows a detail of the upstream part of the combustor used in this study. The upstream part of the combustor, where the fuel spray nozzle is installed, is cylindrical with a diameter of 40 mm and a length of 30 mm. Swirl airflow is supplied from the tangential direction at two points (diameter 2 mm) on the cylinder. The biggest distinguishing feature of this combustor is that, as shown in Figure 1, the fuel nozzle is mounted in the radial direction instead of the axial direction of the combustor. We expected this to further promote fuel–air mixing. Two glow plug ignition devices (NGY, Chino, CA, USA, Y-204TS-1) were installed in the axial direction, which is at the center of the combustor. Additionally, the fuel nozzle (EVERLOY, Osaka, Japan, MMA10) shown in Figure 3 is used as the fuel nozzle, and the kerosene fuel is supplied to the center part, while compressed air to assist fuel spraying is supplied from the nozzle side surface. In the combustion experiment, a fused quartz combustion cylinder with outer diameter 74 mm and length 300 mm was mounted at the lower end of the combustor upstream part.

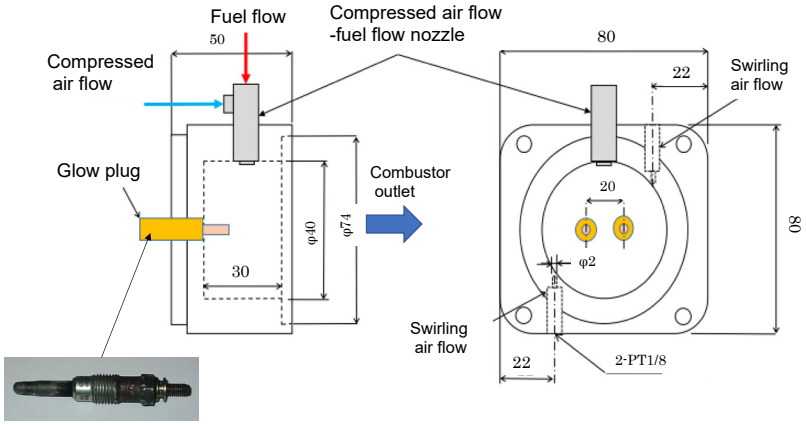

Figure 2. Upstream of the combustor.

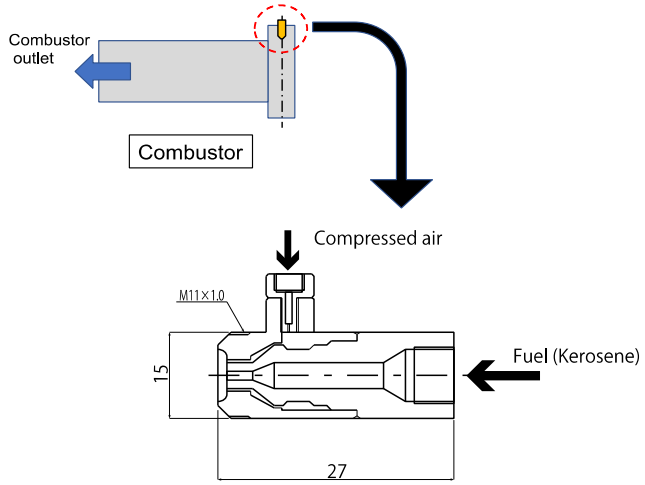

Figure 3. Fuel nozzle (fuel nozzle using compressed air).

This study focuses on the heat source of the HVAF sprayer, which has not received much attention so far, and the flame form formed in the combustor, which is the heat source, changes greatly depending on the mixing ratio of fuel and air supplied. Additionally, we will discuss the temperature change inside the combustor.

Figure 4 shows all of the experimental equipment. The compact combustor used in this experiment consists of a fuel nozzle, a main unit which blows in the swirl airflow, a combustion cylinder, and supporting parts. Kerosene fuel is stored at constant pressure using a pressurization tank employing a compressor, adjusted to the specified flow rate, and supplied to the fuel nozzle. Compressed air for assisting fuel spray and swirl airflow supplied to the combustor are, respectively, pressurized using two compressors, adjusted to the proper pressure with regulators, adjusted to the specified flow rates with flowmeters, and then supplied. For fuel and air, precision valves were used, the fuel flow rate was measured using a Coriolis flow meter (Keyence, Osaka, Japan, FD-SS02A), and the compressed air amount and swirling air amount were measured using a flow meter (Azbil, Tokyo, Japan, MCF0080ARND01). When investigating flame stability in the experiment, photography of flame behavior was carried out with a high-speed camera (KATO KOKEN, Kanagawa, Japan, k7-USB) in order to observe the flame morphology from the combustor side. Additionally, when measuring temperature inside the combustor, the combustion cylinder was switched from fused quartz to SUS. R-type thermocouples of diameter 1.5 mm were inserted into sockets installed in the side of the combustion cylinder at positions 30 mm and 230 mm from the upstream part of the combustor, and data were gathered with a data logger (Keyence, Osaka, Japan, NR-1000) with the sampling time set to 10 msec. Additionally, the direct photograph of the flame was taken using a digital video camera (SONY, Tokyo, Japan, HDR-SR8). To measure the length of the flame, the captured video data were input into a personal computer and the flame was taken from the image data for about 10 s. The lengths were measured and their average was defined as the flame length. In addition, in order to observe the flow field that collides with the curved wall from the fuel injection nozzle inside the combustor, the flow field by the shadow graph method is used for the non-combustion field using a transparent container of the same size that models the actual combustor. Visualization and velocity distribution using particle image velocimetry (PIV) were performed. A laser (KATO KOKEN, Kanagawa, Japan, G1000, 532 nm, 1 W) was used as the sheet light source of the PIV, and the image was taken with a high-speed camera (KATO KOKEN, Kanagawa, Japan, k7-USB).

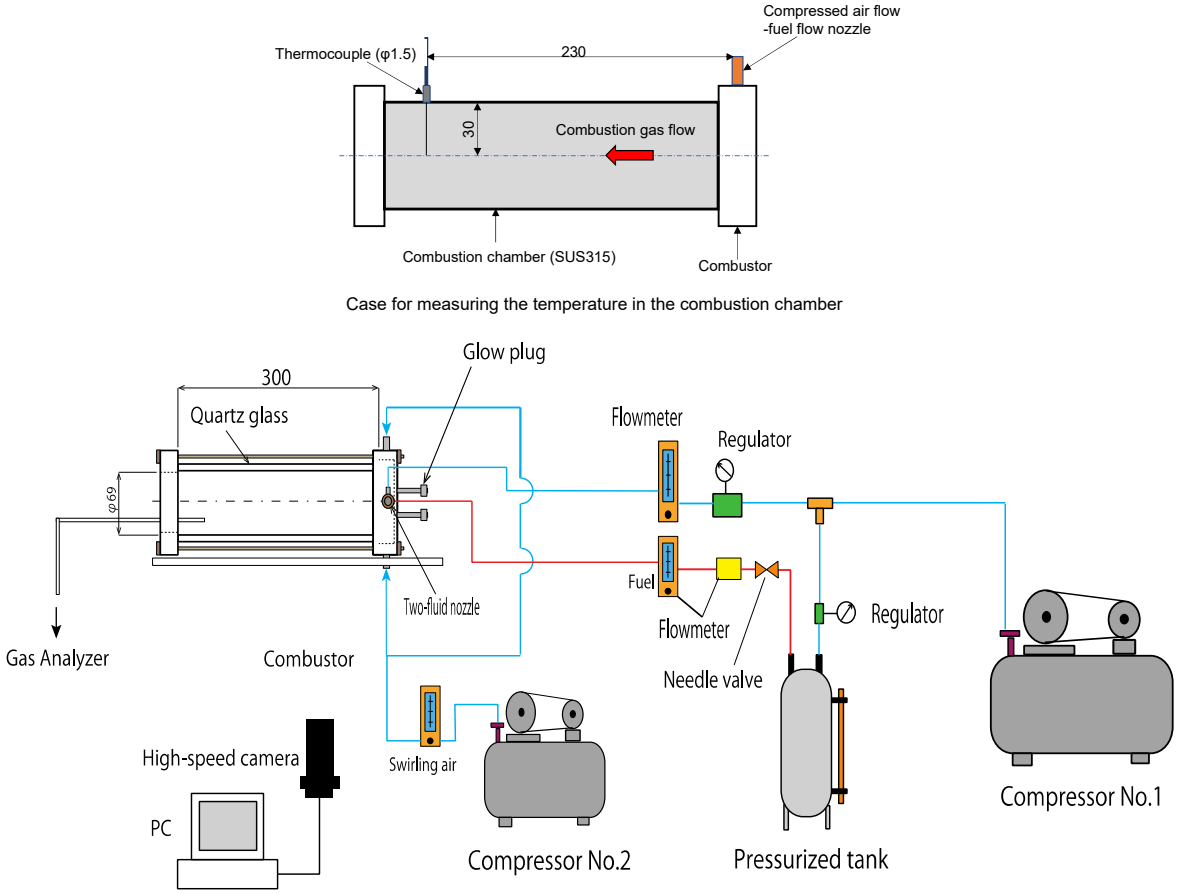

Figure 4. Experimental apparatus.

2.2. Experimental Condition

In all of the experiment conditions, the flow rate of fuel spray assist air was fixed at Q_{air} = 20 L/min. Experiment conditions for each experiment item are indicated below.

(1) In investigating the stable combustion range of flame formed in this combustor after ignition, the fuel flow rate was varied in the range Q_{fuel} = 2–7 mL/min, and the swirl airflow rate was varied in the range Q_{swirl} = 0–70 L/min. The same experiment was performed 5 times near where quenching occurs, and the lower equivalent ratio was recorded. As for the flow rate range of fuel and air, the range in which the flame is formed in this combustor was identified from the preliminary experiment, and the flow rate range was determined from that range.

(2) To ascertain the morphology of flame formed in the combustor, flame observation was performed at each equivalent ratio indicated in (1) above. Flame behavior was photographed with a high-speed camera, and then the average length of flames from the upstream part of the combustor was determined from the captured images.

(3) Proceeding in the same way for temperature in the combustor, data were collected for each equivalent ratio at positions 30 mm and 230 mm in the length direction from the combustor upstream part in order to measure the temperature in the center of the combustor for each equivalent ratio indicated in (1) above. The sampling cycle for this data was 10 ms, and the sampling time was 10 s.

3. Experimental Results

3.1. Visualization of Flow in the Curved Impinging Jet Field

When considering practical use of a combustor, flow near the ignition plugs in the ignition process is crucial, and there is a need to ascertain the flow field inside the burner with this combustor too. However, it is difficult to determine this through experiments

using actual equipment, and thus collision with the combustor wall of fuel sprayed from the fuel injection nozzle was visualized using a container simulating the fuel injection part of the actual equipment.

Figure 5 shows a shadowgraph photo capturing the combustion field in which fuel sprayed from the fuel injection nozzle collides with the curved surface. This figure shows the state at (a) t = 3 ms and (b) t = 10 ms after the start of injection. In the results in Figure 5a, it is evident that the spray flare angle and fuel–air mixture near the curved surface are adequate. Figure 5b, where time has elapsed, shows how the fuel–air mixture has spread throughout the entire inside of the container.

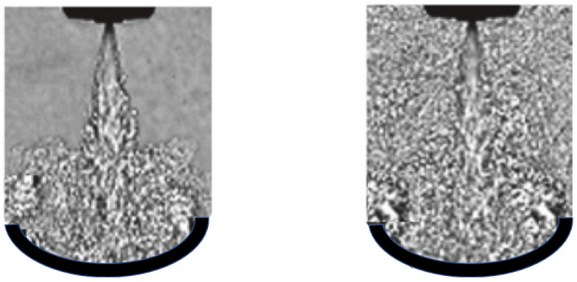

Figure 5. Shadowgraph photo capturing the combustion field in which fuel sprayed from the fuel injection nozzle collides with the curved surface at each time. (**a**) t = 3 ms. (**b**) t = 10 ms.

Figure 6 shows the results when the condition of spray from the fuel injection nozzle was directly photographed, and high-speed measurement was carried out using PIV (Particle Image Velocimetry). Judging from these results, the fuel spray develops, after fuel injection, while involving the surrounding air, and after collision with the wall, the fuel–air mixture curls up. At t = 5.0 ms in particular, it is evident that the fuel–air mixture that has curled up along the wall is entrained again by the spray.

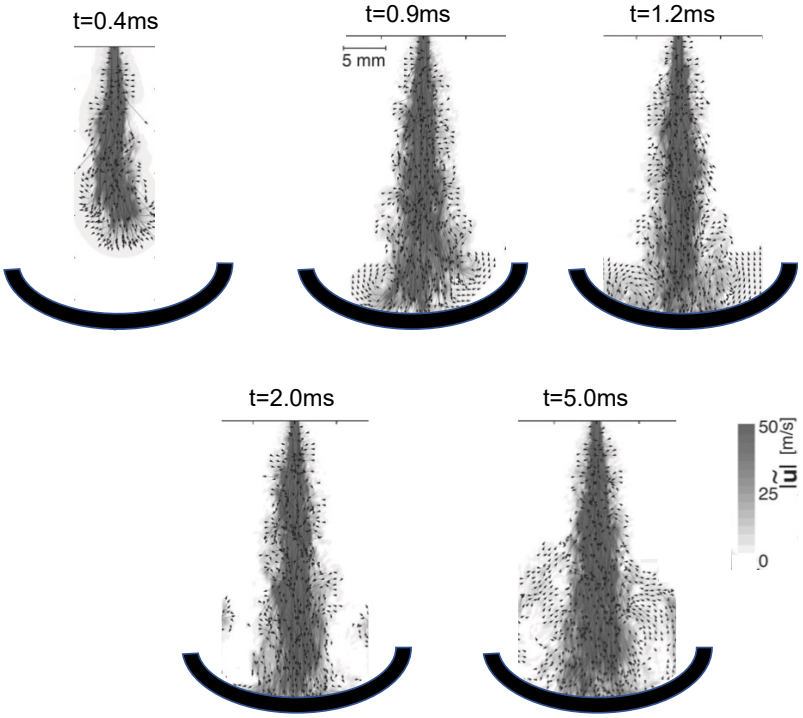

Figure 6. Velocity field of curved impinging spray analyzed by PIV.

3.2. Ignition Characteristics of the Combustor

Ignition of the liquid fuel spray must be reliably realized by providing combustor function. In addition, that ignition happens due to a complex interplay of various factors such as state of the fuel spray, state of the surrounding air, and ignition conditions. If this ignition process is imperfect, the unit will not only fail to fulfill its function as a combustor but there will also be a risk of discharge of toxic unburned gas, and of fire or explosion. Thus, to improve these problems, it will be crucial to quantitatively evaluate ignitability due to fuel spray, and to understand the relationships between ignitability and various parameters which affect it.

With this combustor, the fuel nozzle is mounted in the radial direction of the combustor, and two glow plugs that act as the ignition source are mounted at positions separated by 10 mm on the left and right from the center part in the length direction of the combustor so there is intersection with the fuel spray. In this experiment, we examined the effect on ignition time when we varied the number of glow plugs or their position relative to the center. Figure 7 shows the relationship between glow plug position and time to ignition. The effect of the number of glow plugs is also indicated as a parameter. Additionally, the horizontal axis indicates the glow plug position, and the L = 20 mm position is the center position of the fuel nozzle. As shown in the figure, at the glow plug position L = 20 mm, time to ignition is less than approximately 1 s, but when the glow plug position is moved away from the center part, it is evident that it is hard for the plugs to come into contact with the mixed gas of fuel spray and air, and the time to ignition increases. Additionally, in terms of differences due to the number of glow plugs, two glow plugs have a greater effect on time to ignition than one in the range L = 15–20 mm, but it is evident that, when L < 10 mm, the effect due to the number of glow plugs is smaller. This result shows that the time until ignition is shortened when the glow plug position is near the fuel nozzle center position, but considering practical equipment design, if the glow plug position is near the fuel nozzle center position, a flame is formed in this region, and the glow plug is present within the flame, so the plug is always overheated, and as a result there is a possibility that plug burning deterioration will be hastened; therefore, we want to determine the optimal glow plug position based on the results of these experiments.

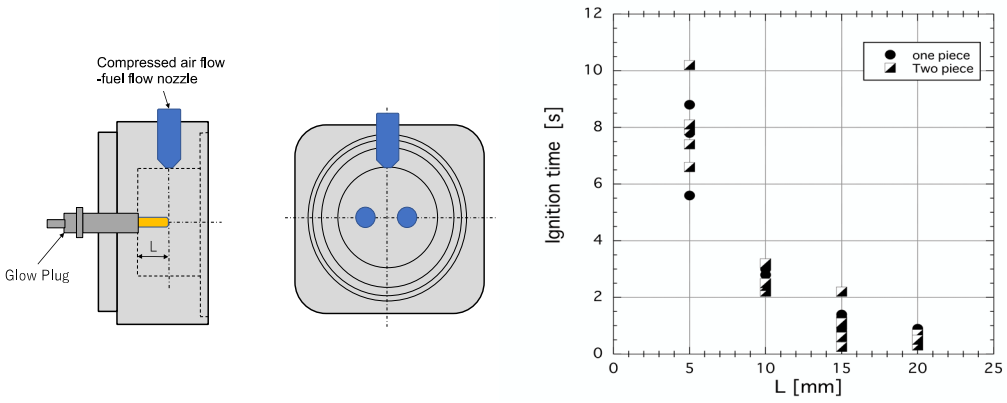

Figure 7. Relationship between glow plug position and time to ignition.

3.3. Flame Stability of the Combustor

Figure 8 shows a flame morphology map for the combustor. The horizontal axis indicates the fuel flow rate (Q_{fuel}) and the vertical axis indicates the swirl airflow rate (Q_{swirl}). The other numerical values given in the figure indicate the equivalent ratio (φ) of the corresponding position. Here, the amount of air used to determine the equivalent ratio defined in this study was the sum of compressed air and swirling airflow. The blue solid line in the figure plots the values where the equivalent ratio decreases, immediately before the flame blows out, and the red solid line plots the values where the equivalent ratio increases, immediately before the flame is quenched in the fuel rich state. Therefore,

the region bounded by the blue solid line and red solid line becomes the combustion region. In this combustion region, a flame with luminous flames that emits soot is formed in the red solid line region where the equivalent ratio is high, and, on the other hand, in the blue solid line region where the equivalent ratio is smaller than one, a flame with blue flames is formed.

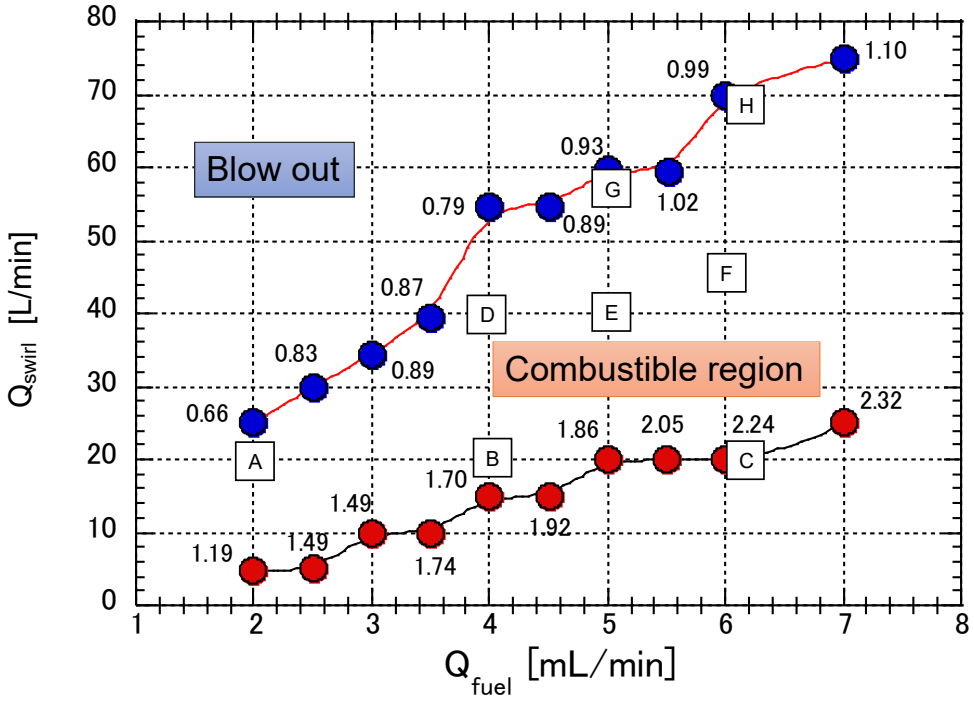

Figure 8. Flame morphology map.

Figure 9 shows a direct photograph (combustion chamber side surface portion and combustion chamber outlet portion) of each equivalent ratio of flames at the positions (**A** to **H**) shown in the flame morphology map of Figure 8. In φ = 0.75 (**A**) in Figure 9a, the luminous flame disappears in the entire flame due to the increase in the swirling air flow rate with respect to the fuel flow rate and, conversely, the blue flame is predominantly formed to the vicinity of the upstream part of the combustor. The flame recedes and the flame length becomes shorter. When φ = 1.33 (**B**) in Figure 9b, the flame transitions from a blue flame to a luminous flame and approaches the combustion limit (lower part), so the flame becomes unstable and begins to vibrate. When φ = 2.20 (**C**) in Figure 9c, the flame is a luminous flame, so the flame becomes a spiral state due to the influence of the swirling air flow and reaches the combustion limit (lower part), so it is in a very unstable state. become. In φ = 1.05 (**D**) in Figure 9d, the luminous flame is mixed in the blue flame, but it is in a very stable state. In φ = 1.20 (**E**) in Figure 9e and φ = 1.45 (**F**) in Figure 9f, the luminous flame gradually becomes dominant, and the length of the flame also extends downstream of the combustor. Furthermore, at φ = 0.96 (**G**) in Figure 9g and φ = 1.02 in Figure 9h, the flame appears in the blue flame behind the luminescent flame, but it is approaching the combustion limit (upper part). The flame oscillates in the length direction. For the above reasons, it was confirmed that the swirling air flow is an important parameter for stabilizing the flame.

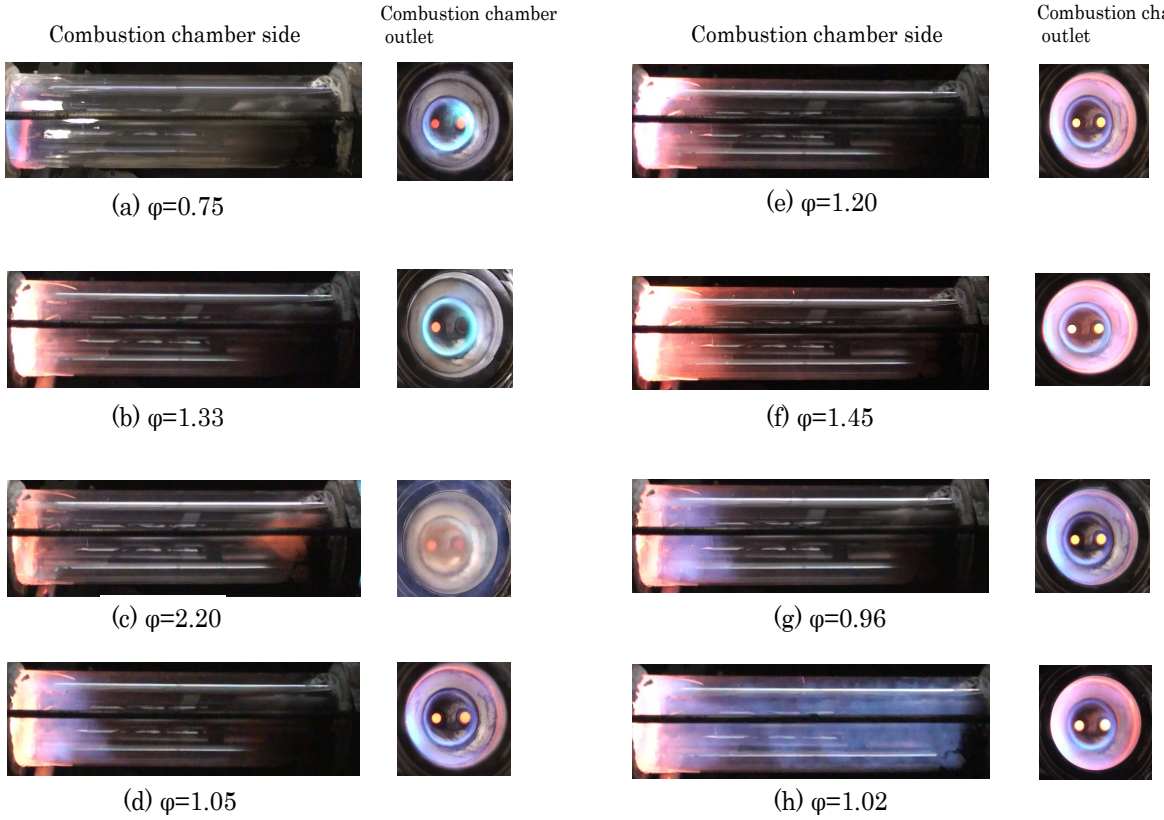

Figure 9. Direct photo of these typical flames.

3.4. Transition Flame and Temperature Fluctuations in the Combustion Chamber

From the combustion state with a stable blue flame where no soot is produced, the swirl airflow rate begins to change due to external factors, and it is advantageous from a practical standpoint to understand the process whereby combustion becomes unstable, i.e., the combustion behavior of the transition flame. Thus, as shown in the flame map indicated in Figure 10, temperature changes and flame morphology inside the combustor were observed for regions A, B, and C when the fuel flow rate Q_{fuel} was fixed at 4, 5, or 6 mL/min, and the swirl airflow rate Q_{swirl} was varied in the range 15–60 L/min.

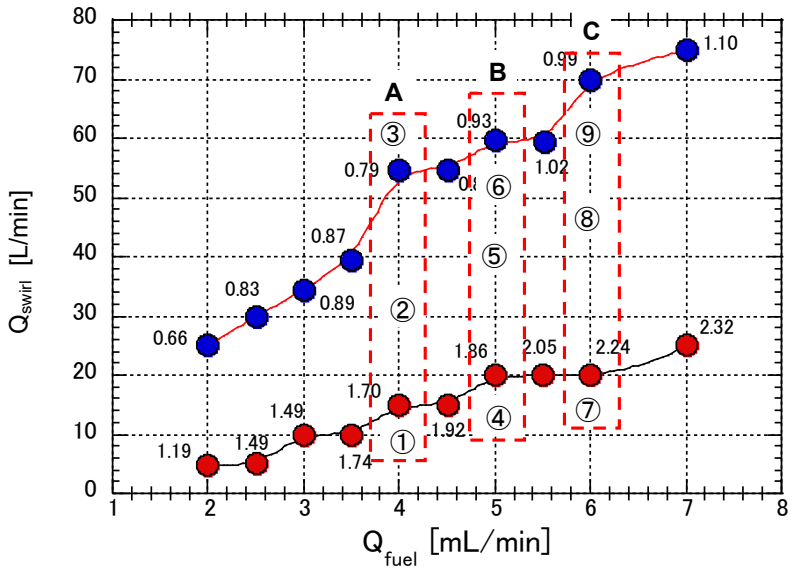

Figure 10. Direct photo of these typical flames.

First, focus on region A in which Q_{swirl} is changed by fixing it at Q_{fuel} = 4 mL/min. Figure 11 shows a direct photograph of the flame and temperature fluctuations at each point in region A. Figure 11a shows the result of Q_{swirl} = 15 L/min (φ = 1.70). This point is near the limit of the red solid line region where the equivalent ratio is high, as shown in Figure 10. This flame periodically oscillates and burns in the axial direction. When the flame stays in the upstream part of the combustor, it is a blue flame, but when the flame extends to the downstream part, it changes to a flame in which a luminous flame is mixed. The temperature in the combustion chamber in this flame state is stagnant at around 600 °C. Figure 11b shows the result of Q_{swirl} = 35 L/min (φ = 1.08). In the flame state, the vibration combustion shown above is cured, and the flame is stagnant in the state of blue flame in the upstream part of the combustor and is burning stably. It can be seen that the temperature in the combustion chamber at this time is gradually rising because the flame is stagnant. Figure 11c shows the result of Q_{swirl} = 55 L/min (φ = 0.79). The flame morphology shows a blue flame near the upstream part of the combustor, but the flame gradually extends to the downstream side, and the color of the flame becomes lighter. The temperature in the combustion chamber in such a flame state tends to gradually decrease.

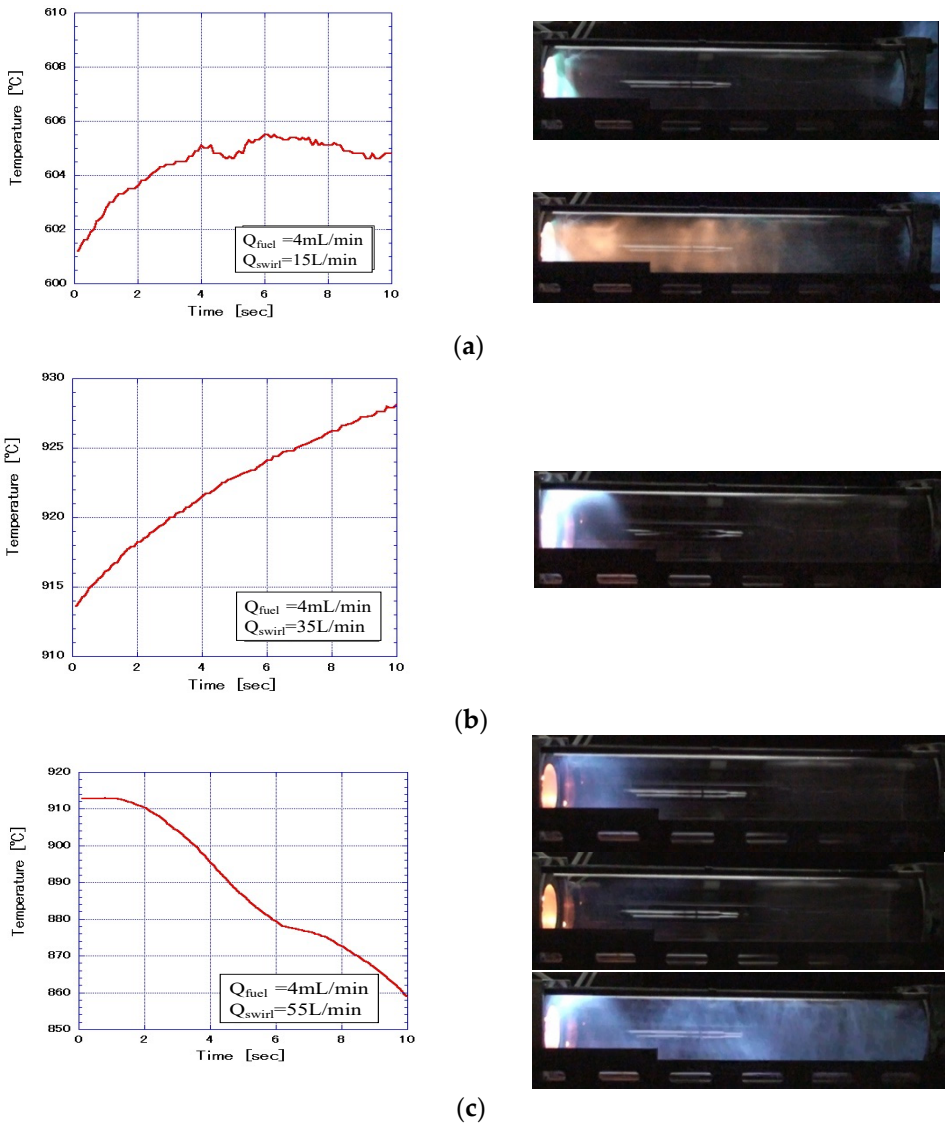

Figure 11. Temperature fluctuation in the combustion chamber (Q_{fuel} = 4 mL/min fixed). (**a**) Q_{swirl} = 15 L/min. (**b**) Q_{swirl} = 35 L/min. (**c**) Q_{swirl} = 55 L/min.

Next, focus on region B where Q_{swirl} is changed by fixing Q_{fuel} = 5 mL/min. Figure 12 shows a direct photograph of the flame and temperature fluctuations at each point in region B. Figure 12a shows the result of Q_{swirl} = 15 L/min (φ = 1.86). Since this point is near the limit of the red solid line region as in Figure 11a, the flame is very unstable. In this region, blue flames and luminous flames extending to the downstream part of the combustor repeatedly appear while vibrating, and then a small explosion occurs near the upstream part. At this time, the temperature in the combustion chamber rises when the flame is present but, once the flame disappears, the temperature decreases. Figure 12b shows the result of Q_{swirl} = 40 L/min (φ = 1.24). The flame morphology at this time is similar to that in Figure 11b, and it can be seen that the flame stagnates in the state of blue flame in the upstream part of the combustor and burns stably. Therefore, the temperature in the combustion chamber is gradually rising. Figure 12c shows the result of Q_{swirl} = 60 L/min (φ = 0.93). The flame morphology shows the same flame behavior as in Figure 11c. Therefore, the temperature in the combustion chamber at this time also tends to gradually decrease.

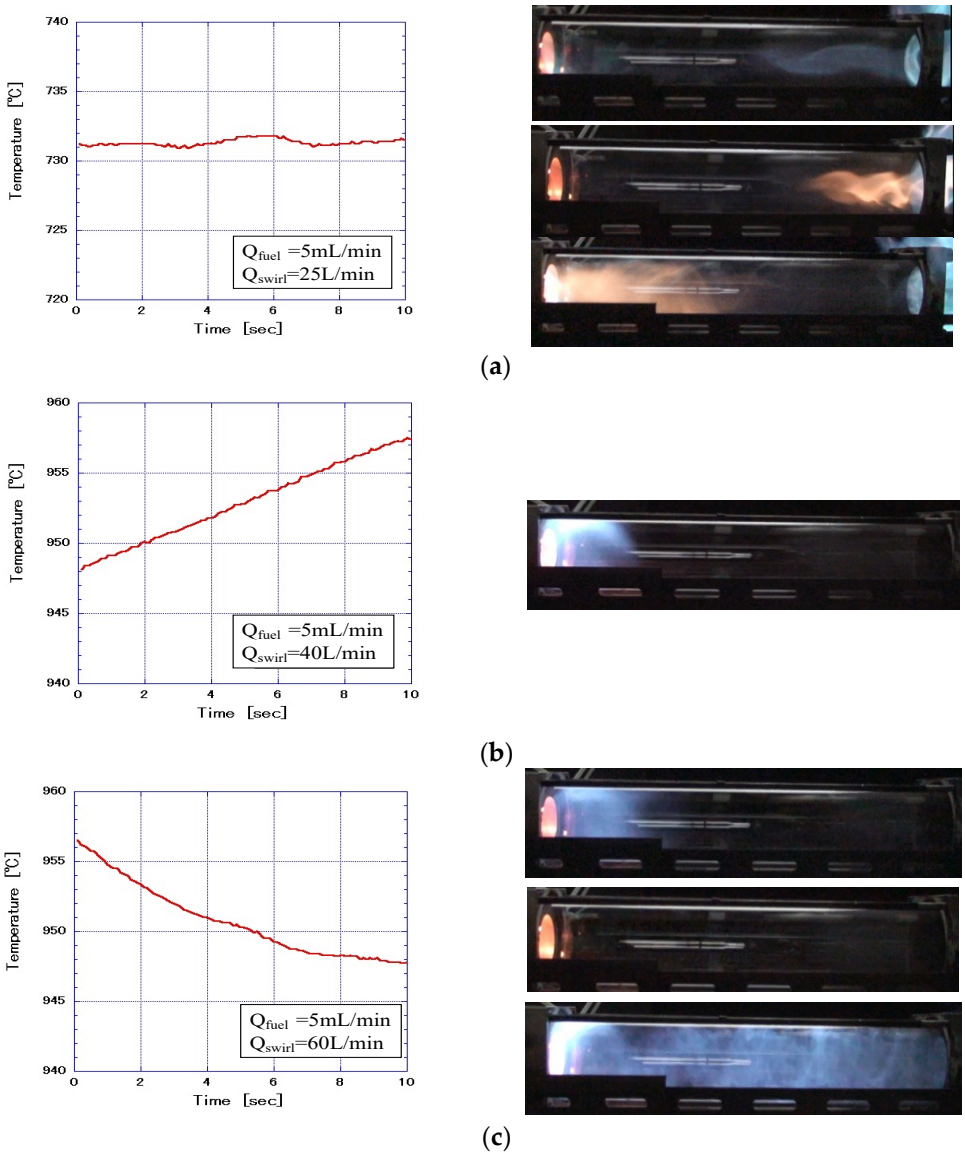

Figure 12. Temperature fluctuation in the combustion chamber (Q_{fuel} = 5 mL/min fixed). (**a**) Q_{swirl} = 25 L/min. (**b**) Q_{swirl} = 40 L/min. (**c**) Q_{swirl} = 60 L/min.

Furthermore, the region C where Q_{fuel} = 6 mL/min is fixed and Q_{swirl} is changed is examined. Figure 13 shows a direct photograph of the flame and temperature fluctuations at each point in region C. Figure 13a shows the result of Q_{swirl} = 20 L/min (φ = 2.24). Since this point has the same flame behavior as described above in Figures 11a and 12a, the temperature fluctuation inside the combustor is also similar. Figure 13b shows the result of Q_{swirl} = 45 L/min (φ = 1.38). As for the flame morphology in this state, as shown in Figures 11b and 12b, the flame is stable in the state of blue flame in the upstream part of the combustor, so the temperature in the combustion chamber also rises gradually. Figure 13c shows the result of Q_{swirl} = 60 L/min (φ = 1.12). Since this point has not yet reached the blue solid line region, as shown in Figure 10, the flame fluctuates slightly in the axial direction of the combustor but remains relatively stable. Therefore, the temperature in the combustion chamber fluctuates up and down as the flame repeatedly moves in the axial direction of the combustor.

From the above results, it can be seen that the flame behavior formed in the combustor due to the change in the swirling air flow has a great influence on the temperature inside the combustor, and the approximate temperature change is determined by the form of the flame morphology.

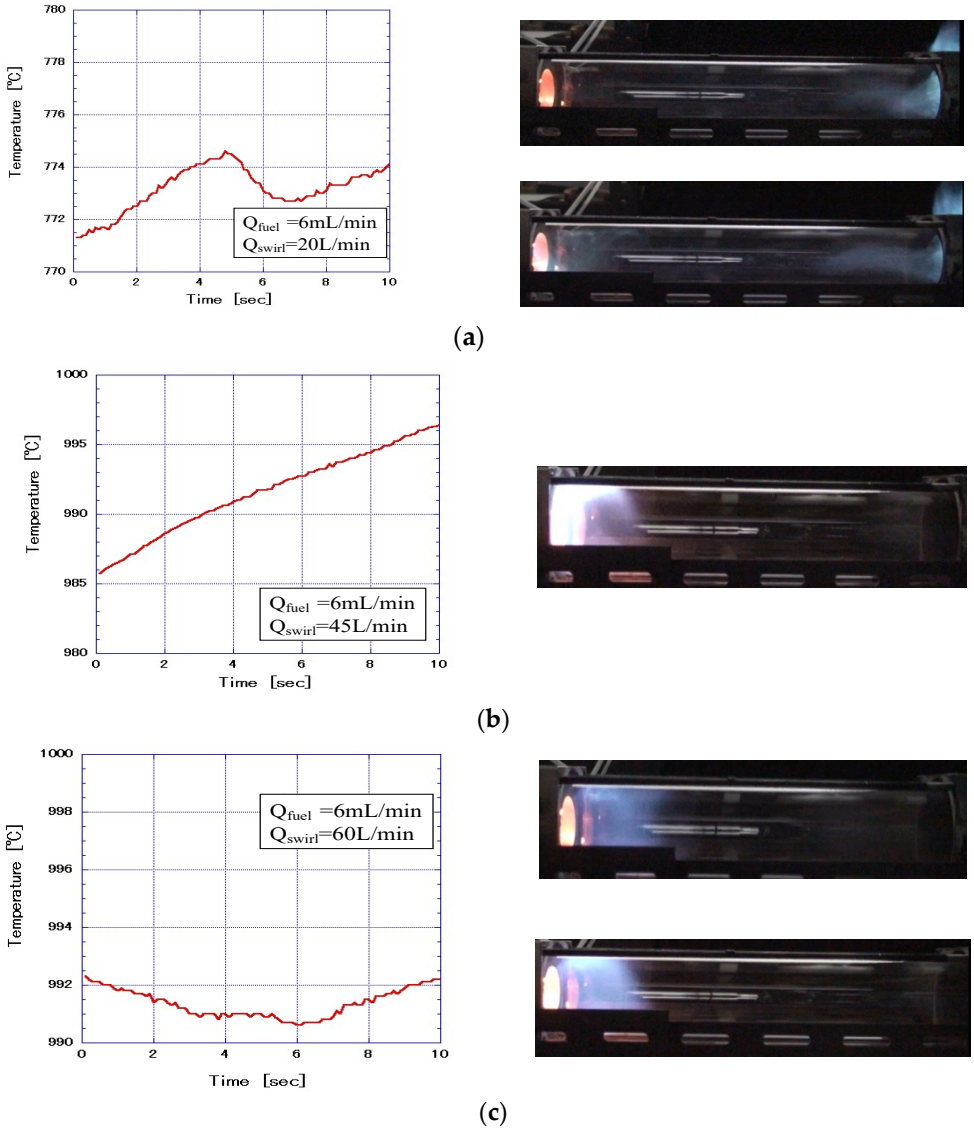

Figure 13. Temperature fluctuation in the combustion chamber (Q_{fuel} = 6 mL/min fixed). (**a**) Q_{swirl} = 20 L/min. (**b**) Q_{swirl} = 45 L/min. (**c**) Q_{swirl} = 60 L/min.

3.5. Effects of the Equivalent Ratio Variation on Flame Length and Temperature in the Combustion Chamber

When a combustor is considered as a heat source for thermal spraying, the temperature produced at the heat source part is extremely important. This becomes a crucial factor for determining the melted and semi-melted state of the thermal spray material, and has a major impact on coating performance. On the other hand, the temperature in the combustion chamber has a major effect on flame morphology, as described above, and here we varied the equivalent ratio, and examined effects on flame length and temperature in the combustion chamber.

First, we examined the effect of changes in the equivalent ratio on flame length. Figure 14 shows the relationship between the equivalent ratio and flame length when, as parameters, swirl airflow Q_{swirl} is fixed at 20, 30, 40, and 50 L/min, and the fuel flow rate Q_{fuel} is varied. It was found that, when the equivalent ratio is increased, the flame suddenly begins to extend at around φ = 1.16 with Q_{swirl} = 20 L/min, at φ = 1.5 with Q_{swirl} = 30 L/min, and around φ = 1.6 with Q_{swirl} = 40 L/min. Overall; when the flame is backed up in the upstream part (L < 100 mm), the swirl airflow is more dominant than the fuel flow rate, and thus the flame formed in the combustor is in the blue flame state but when the flame extends, luminous flames mix in with the blue flames and, as the equivalent ratio increases, so does the ratio of luminous flame. Due to the relationship between the equivalent ratio φ and the flame length shown in Figure 14, the flame length changes sharply from a specific equivalent ratio φ in general; until the equivalent ratio is around one, the flame is a premixed flame. It forms a blue flame, which stagnates upstream of the combustor. After that, when the equivalent ratio is increased, the bright flame is mixed in the blue flame, and the flame becomes unstable by transitioning from the premixed flame to the diffuse flame. It is considered that the length of the flame extends to the downstream side at this time because the fuel that could not be burned in the upstream part of the combustor moves to the downstream side and combustion occurs there. Furthermore, if the swirling air flow, which is a variable, is increased, the flame is maintained in the upstream part of the combustor even if the equivalent ratio is high, so it is considered that the rapid change in the flame length is delayed.

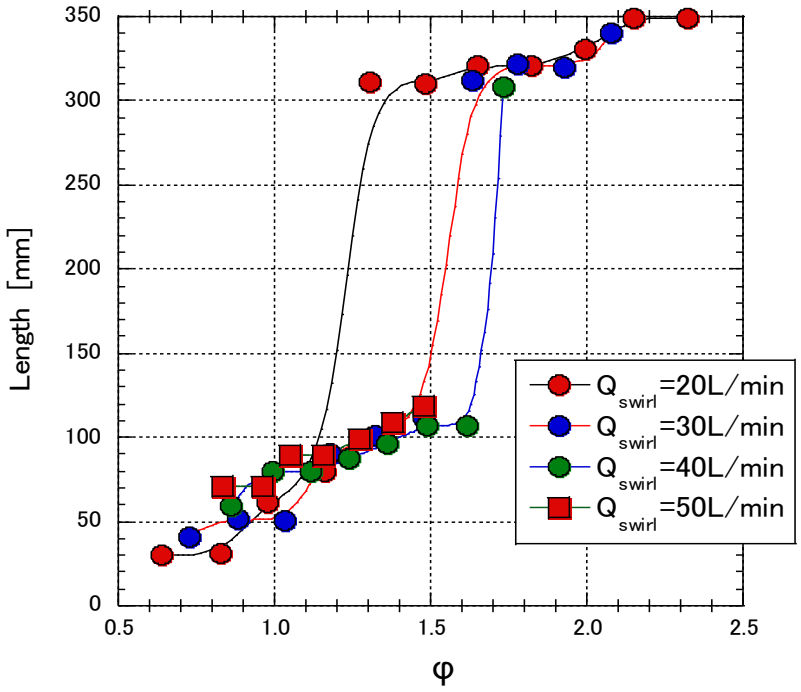

Figure 14. Relationship between equivalent ratio and flame length when the fuel flow rate Qfuel is changed.

Figure 15 shows the relationship between the equivalent ratio, and the combustion chamber internal temperature and flame length, when fixing at Q_{fuel} = 6 mL/min while varying Q_{swirl}. Representative photos of the flame morphology are also shown in the figure. The position for measurement of temperature in the combustion chamber is 30 mm downstream from the upstream part of the combustion chamber, and 5 mm from the combustion chamber wall in the radial direction; for the temperature measurement value, we time averaged data collected at 10 s intervals with a sampling cycle of 10 ms. Furthermore, for the measurement value of flame length, photos of flame behavior were taken at 1 s intervals with a high-speed camera, and flame length was determined from the captured image data and then averaged to obtain the final value. When the equivalent ratio φ is increased, the flame gradually extends to the combustor downstream side, and from around φ = 1.5 the flame suddenly extends to the downstream side and begins to vigorously pulsate. Regarding the temperature near the wall of the combustion chamber corresponding to this flame behavior, on the other hand, the flame is backed up in the combustor upstream part up to φ < 1.5 and, due to the effects of swirl airflow, the flame fluctuates near the wall of the combustion chamber, and thus the temperature exhibits a value of approximately 1000 °C. However, when φ > 1.5, it is evident that the effects of the swirl airflow diminish, and flames concentrate overall in the center direction, so there is a sudden decrease in temperature near the combustion chamber.

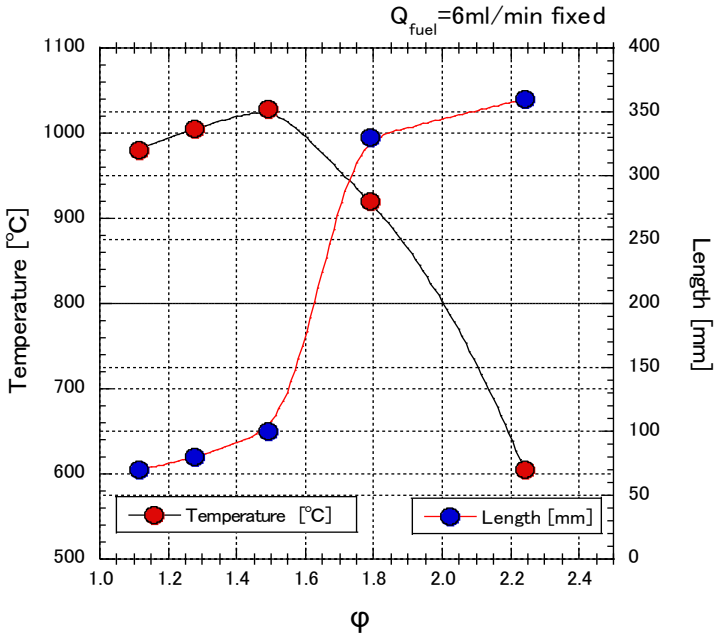

Figure 15. Relationship between the equivalent ratio when the swirling air flow is changed, the combustion chamber temperature, and the flame length (Q_{fuel} = 6 mL/min fixed).

Next, Figure 16 shows the relationship between the equivalent ratio, and the combustion chamber internal temperature and flame length, when fixing Q_{swirl} = 20 L/min and varying Q_{fuel}. Just as when Q_{swirl} was varied while Q_{fuel} was kept fixed, as shown in Figure 15, there was a sudden increase starting near φ = 1.2, and a gentle increase thereafter. On the other hand, the temperature near the combustion chamber wall increases with increasing φ and peaks at φ = 1.16. After that, the temperature switches to a declining trend. These results are the same as those for flame length and variation in temperature near the combustion chamber wall shown in Figure 14, but when flame behavior is observed for φ in the range 1.16 < φ < 1.5, the flame moves from the combustion chamber wall to the combustion chamber center due to the increase in Q_{fuel}; thus, it is thought that the temperature near the combustion chamber wall suddenly starts to decrease.

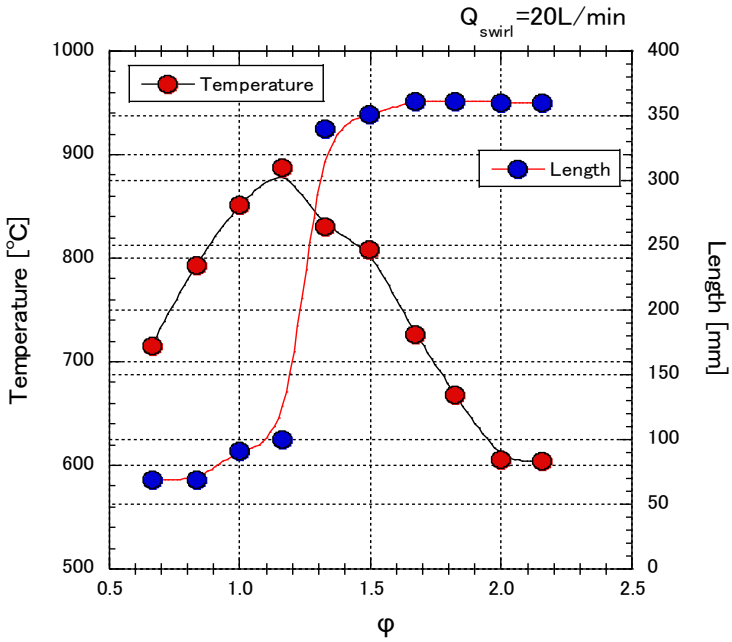

Figure 16. Relationship between the equivalent ratio when the fuel flow is changed, the combustion chamber temperature, and the flame length (Q_{swirl} = 20 L/min fixed).

For the above reasons, the change in the equivalent ratio becomes a factor determining the dominance of fuel flow or swirl airflow in the narrow combustion chamber and, for this reason, flame behavior varies greatly; thus, it was found that the temperature in the combustion chamber is also affected.

4. Conclusions

In this study, we developed a compact combustor with a narrow channel near the actual combustion field as a heat source for HVAF thermal spray equipment. Using this combustor, we carried out a detailed investigation of stability of the flame formed by this combustor, flame morphology, and temperature behavior inside the combustion chamber. We also determined the stable combustion range where soot is not produced in the practical combustion field, and examined operating parameters needed for combustion control. As a result, the following findings were obtained.

(1) Regarding the position of the glow plugs considered as an ignition source for the combustor, the time to ignition is shortened near the center position of the fuel nozzle; however, if the glow plug position is near the fuel nozzle center, there is a possibility of burning deterioration, and thus, when considering practical design, we believe it is best to divide it into a pilot combustion section and a main combustion section.

(2) The magnitude of the swirl airflow has a major effect on structure of the flame formed in the combustor, and we were able to determine the stable combustion range of the combustor.

(3) As the swirling air flow rate changes, the equivalent ratio of the entire combustor changes significantly, and the flame structure also transition from the premixed flame to the diffusion flame. From this study, it was confirmed that the temperature inside the combustor has a great influence on the flame structure.

Author Contributions: Conceptualization and methodology, H.K. and K.O.; formal analysis, validation, investigation, and data curation: H.K. and K.F.; writing—original draft preparation and visualization, H.K.; writing—review and editing, supervision, and project administration, H.K., E.M. and K.M. All authors have read and agreed to the published version of the manuscript.

Funding: This research received no external funding.

Conflicts of Interest: The authors declare no conflict of interest.

References

1. Vijay, S.; Wang, L.; Lyphout, C.; Nylen, P.; Markocsan, N. Surface characteristics investigation of HVAF sprayed cermet coatings. *Appl. Surf. Sci.* **2019**, *493*, 956–962. [CrossRef]
2. Kowalsky, K.A.; Marantz, D.R.; Smith, M.F.; Oberkampf, W.L. HVOF: Particle, Flame Diagnostics and Coating Characteristics. In *Proceedings of the thermal spray conference and exposition, Long Beach, CA, USA, 21–24 May 1990*; U.S. Department of Energy: Oak Ridge, TN, USA, 1990; SAND-90-0844C.
3. Hasui, A. *Thermal Spray Engineering*; Sanpo Pub: Tokyo, Japan, 1996; pp. 209–259. (In Japanese)
4. Wada, T. Current status and problems of HVOF thermal spray. *J. Surf. Finish. Soc. Jpn.* **2008**, *59*, 495–500. (In Japanese) [CrossRef]
5. Hagerty, W.W.; Shea, J.F. A study of the stability of plane fluid sheets. *J. Appl. Mech.* **1955**, *22–24*, 509–514. [CrossRef]
6. Fraser, R.P.; Eisenklam, P.; Dombrowski, N.; Hasson, D. Drop formation from rapidly moving liquid sheets. *AIChE J.* **1962**, *8*, 672–680. [CrossRef]
7. Dombrowski, N.; Hooper, P.C. The effect of ambient density on drop formation in sprays. *Chem. Eng. Sci.* **1962**, *17*, 291–305. [CrossRef]
8. Fukui, N.; Sato, G. Investigation of impinging atomization. *Trans. JSME* **1971**, *37*, 1735–1745. (In Japanese) [CrossRef]
9. Tokuoka, N.; Sato, G. Investigation of impinging atomization. *Trans. JSME* **1977**, *43*, 3444–3454. (In Japanese) [CrossRef]
10. Tanasawa, Y.; Sasaki, S.; Nagai, N. Atomization of liquids by means of flat impingement. *Tech. Rep. Tohoku Univ.* **1957**, *22*, 73–95.
11. Inamura, T.; Saito, T.; Tomoda, T. Modeling of Spray Formation in Wall Impingement Type of Injector. *Proc. Acad. Lect. (Spring) Soc. Automot. Eng. Jpn.* **2002**, *2002*, 423–426.
12. Inamura, T.; Nagai, N.; Sunanaga, H.; Masubuchi, M. The behavior of a liquid film formed by an impinging jet on a solid wall (1st Report, Thickness distribution in a liquid film formed by a single obliquely impinging jet). *Trans. JSME B* **1991**, *57*, 1327–1331. (In Japanese) [CrossRef]
13. Inamura, T.; Nagai, N.; Masubuchi, M. The behavior of a liquid film formed by an impinging jet on a solid wall (2st Report, Interaction between liquid films generated by two impinging jets at a right angle on the wall). *Trans. JSME B* **1991**, *57*, 1332–1339. (In Japanese) [CrossRef]
14. Shiga, S.; Araki, M.; Horikoshi, J.; Yamada, H.; Hayashi, S.; Nakamura, H.; Obokata, T. Effect of wall impingement on the atomization characteristics of an air-blasting nozzle for jet engines. *Proc. ICLASS* **2003**, *2003*, 232–237.
15. Araki, M.; Horikoshi, J.; Yamada, H.; Shiga, S.; Hayashi, S.; Nakamura, H.; Obokata, T. Wall geometry effects on atomization characteristics of an impingement jet type jet engine fuel injector. *Trans. JSME B* **2005**, *71*, 2568–2574. (In Japanese) [CrossRef]
16. Karasawa, T.; Tanaka, M.; Abe, K.; Shiga, S.; Kurabayashi, T. Effect of nozzle configuration on the atomization of a steady spray. *At. Sprays* **1992**, *2*, 411–426. [CrossRef]
17. Menghini, D.; Marra, F.S.; Allouis, C.; Beretta, F. Effect of excess air on the optimization of heating appliances for biomass combustion. *Exp. Therm. Fluid Sci.* **2008**, *32*, 1371–1380. [CrossRef]
18. Qian, X.; Lee, S.; Chandrasekaran, R.; Yang, Y.; Caballes, M.; Alamu, O.; Chen, G. Electricity Evaluation and Emission Characteristics of Poultry Litter Co-Combustion Process. *Appl. Sci.* **2019**, *9*, 4116. [CrossRef]
19. Qian, X. Statistical Analysis and Evaluation of the Advanced Biomass and Natural Gas Co-Combustion Performance. Ph.D. Thesis, Morgan State University, Baltimore, MD, USA, 2019.